arXiv:1612.03948v2 [cs.LG] 3 Mar 2017

Machine learning approach for identification of release sources in advection-diffusion systems

Valentin G. Stanev

Physics and Chemistry of Materials Group
Theoretical Division
Los Alamos National Laboratory
Los Alamos, NM, USA

Filip L. Iliev

Physics and Chemistry of Materials Group
Theoretical Division
Los Alamos National Laboratory
Los Alamos, NM, USA

Velimir V. Vesselinov

Computational Earth Science Group
Earth and Environmental Sciences Division
Los Alamos National Laboratory
Los Alamos, NM, USA

Boian S. Alexandrov*

Physics and Chemistry of Materials Group
Theoretical Division
Los Alamos National Laboratory
Los Alamos, NM, USA

Abstract

Mathematically, the contaminant transport in an aquifer is described by an advection-diffusion equation and the identification of the contamination sources relies on solving a complex ill-posed inverse model against the available observed data. The contaminant migration is usually monitored by spa-

*Corresponding author
Email address: boian@lanl.gov (Boian S. Alexandrov)

tially discrete detectors (e.g. monitoring wells) providing temporal records representing sampling events. These records are then used to estimate properties of the contaminant sources, e.g., locations, release strengths and model parameters representing contaminant migration (e.g., velocity, dispersivity, *etc.*). These estimates are essential for a reliable assessment of the contamination hazards and risks. If there are more than one contaminant sources (with different locations and strengths), the observed records represent contaminant mixtures; typically, the number of sources is unknown. The mixing ratios of the different contaminant sources at the detectors are also unknown; this further hinders the reliability and complexity of the inverse-model analyses. To circumvent some of these challenges, we have developed a novel hybrid source identification method coupling machine-learning and inverse-analysis methods, and called Green-NMFk. It performs decomposition of the observed mixtures based on Non-negative Matrix Factorization method for Blind Source Separation, coupled with custom semi-supervised clustering algorithm, and uses Green's functions of advection-diffusion equation. Our method is capable of identifying the unknown number, locations, and properties of a set of contaminant sources from measured contaminant-source mixtures with unknown mixing ratios, without any additional information. It also estimates the contaminant transport properties, such as velocity and dispersivity. Green-NMFk is not limited to contaminant transport but can be applied directly to any problem controlled by partial-differential parabolic equation where mixtures of an unknown number of physical sources are monitored at multiple locations. Green-NMFk can be also applied with different Green's functions; for example, representing anomalous (non-Fickian) dispersion or wave propagation in dispersive media.

Keywords: Non-negative matrix factorization; Robustness analysis; Semi-supervised learning; Groundwater contamination; Source identification; Advection-diffusion transport

---

1. Introduction

For several decades, one of the most important research topics in the hydrological sciences has been the contaminant transport in subsurface environment [1, 2]. The research has been driven by substantial challenges associated with prediction and remediation of contaminant plumes in natural environment. Most of these challenges are due to uncertainties associated

with contaminant sources (e.g. source locations, emission strengths, release transients, etc.) as well as contaminant migration (e.g., velocity, dispersivity, etc., related to aquifer and contaminant transport properties). To determine the number of the contaminant sources, their locations and the physical properties impacting contaminant plume behavior from a set of observations, collected at multiple locations and times, is an important task that can yield important information much needed for contaminant fate and transport predictions, hazard and risk assessments, and remediation. Most often, the information about contamination sources and contaminant migration in an aquifer is limited or not available, which explains the increasing use of complex numerical inverse model analyses [3, 4, 5, 6, 7, 8] and multivariate statistical and machine learning techniques [9, 10, 11, 12, 13] utilized in response to the need of accurate predictive approaches of perpetually increasing number of environmental management problems caused by contamination groundwater-supply resources [14].

The existing methods for contaminant source identification, for calibration and validation, rely (in some form) on available contamination site observations. The tools for observation of contaminant plume are various types of detector (sensor) arrays recording spatiotemporal behavior of the contaminant plumes. The detectors are typically monitoring wells.

Importantly, these detectors typically measure mixtures of signals originating from unknown number of contaminant sources, which presents an additional challenge. If the original contaminant signals causing the observed mixed contaminant plumes can be successfully "unmixed", then decoupled physics (geochemical) models may be applied to analyze the propagation of each contaminant independently.

In this paper we present a new hybrid method, which we call Green-NMFk, for identification of unknown sources. Green-NMFk is utilizing (a) the Green's function of the corresponding partial-differential equation, in the case of contaminant transport it is advection-diffusion equation, (b) a Blind Source Separation (BSS) technique [15], based on Non-Negative Matrix Factorization (NMF) [16], combined with a custom made semi-supervised clustering algorithm [17], to unmix the observations and identify the contaminant sources, and (c) Akaike Information criterion.

Using synthetic data, we demonstrate that Green-NMFk is capable of accurately determining the unknowns: number, locations, and physical characteristics of a set of unknown contaminant sources from observed samples of their mixtures, without any additional information about the sources or

physical properties of the medium where the contaminant transport occurs. Furthermore, the method also estimates the contaminant transport properties of the medium, such as advective transport velocity, and dispersivity.

By combining model-free machine BSS approach with inverse-problem analysis we are able to solve problems, which present challenge for usual BSS methods, but are very common in practical applications: signals that change their form with time, either because of the fundamental nature of the propagation process, or because of the properties of the media.

2. Statement of the problem

The main goal of the paper is to present a novel hybrid method, which we call Green-NMFk, that combines the Green's function of the advection-diffusion equation with a semi-supervised adaptive machine learning approach for identification of contaminant sources in porous media, based on a set of observations. We assume that the observations are taken at several detectors, dispersed in space, and monitoring contaminant transient over a representative period of time. When there are multiple contamination sources in the aquifer each detector registers a mixture of contamination fields (plumes) originating from different sources (release locations). It is assumed that each contaminant source is releasing the same geochemical constituent that is mixed in the aquifer and the resultant mixture is detected at the observation points (detectors). If each source was releasing different geochemical constituents, the analyses will be somewhat simpler and different; however, similar methodology can be applied with minor adjustments. Our objective is to identify the unknown number, release locations and physical parameters of the original contamination sources, which requires first to decompose the recorded mixtures to their original components. This decomposition allows us to use the Green's function of the advection-diffusion equation to extract the physical parameters, location coordinates and time dependence of the sources. In the rest of this section, we present the general mathematical formulation of the problem, and introduce the notations we are going to use.

2.1. Advection-diffusion equation

At equilibrium, the mathematical description of transport of solute in a medium can be derived by the general principle of conservation of mass by applying the continuity equation [18]. In its general form, this transport is

described by linear partial-differential parabolic equation:

$$\frac{\partial C}{\partial t} = \nabla(\mathbf{D} \cdot \nabla C) - \nabla \cdot (\mathbf{u}C) + LC + Q. \quad (1)$$

This equation describes the rate of change of the concentration of the solute/contaminant $C(\mathbf{x}, t)$, defined in some (space and time) domains: $\mathbf{x} \in \mathbb{R}^d$ and $t \in [t_{init}, t_{final}]$. The matrix $\mathbf{D}$ is the hydrodynamic dispersion, which is a combination of molecular diffusion and mechanical dispersion (in porous media the latter typically dominates). While the diffusion part of the matrix $\mathbf{D}$ is diagonal, the dispersion is generally not. The advective velocity $\mathbf{u}$ (also known as pore velocity, representing Darcy groundwater flow velocity divided by medium porosity) is caused by the bulk motion of the fluid in the aquifer. Q is the source strength function, representing possible sinks and sources of the contaminants. The term involving L describes possible chemical transformations of the contaminant. In the following, we will neglect this term, assuming that $L = 0$. Note that this type of equation also describes heat transport in various media (with or without convection) [19], and the exact procedure presented here can be applied to this problem as well.

For simplicity, we will consider a (quasi-)two-dimensional medium, so $\mathbf{x} \in \mathbb{R}^2$, and we assume that z is a constant, $z = z_0$. We also make two additional simplifying approximations. The first is that $\mathbf{u}$ is uniform, $\nabla \cdot \mathbf{u} = 0$ (although $\mathbf{u}$ remains unknown), so we can simplify Eq.1 by choosing the advection velocity to be along the x-axis. The second is that $\mathbf{D}$ is uniform (does not depend on the coordinates), which allows to rewrite Eq.1 as:

$$\frac{\partial C}{\partial t} = \nabla(\mathbf{D} \cdot \nabla C) - \nabla \cdot (\mathbf{u}C) + Q \equiv D_x \frac{\partial^2 C}{\partial x^2} + D_y \frac{\partial^2 C}{\partial y^2} - u_x \frac{\partial C}{\partial x} + Q. \quad (2)$$

Note that although the molecular diffusion usually obeys $D_x^{diff} = D_y^{diff}$, due to the presence of mechanical dispersion, we have: $D_x \neq D_y$, because the advection motion breaks the isotropy of space. We will consider Q to be a collection of point sources localized in both space and time, so it can be written as: $Q \sim \sum Q_s \delta(x - x_s)\delta(y - y_s)\delta(t - t_s)$, where the index s specifies the coordinates and the release time of the s-th contaminant source. Here $\delta(...)$ denotes Dirac delta-function [20], We assume the sources are points in space and the contaminant mass release is instantaneous at time.

To uniquely specify a solution of Eq.2, we need to impose initial and boundary conditions. We also assume that these is no contamination before

the sources start emitting, and the initial condition is $C(t < \min(t_s)) = 0$. The choice of boundary conditions is more complicated, and either Dirichlet, Neumann or Cauchy boundary conditions can be appropriate, depending on the specific details for a given site problem. For simplicity, we will concentrate on the case of an infinite two-dimensional space, assuming that the aquifer is large enough so its boundaries do not affect the distribution of C, at least at the time-scales of interest. In this case, we can choose for a boundary condition at infinity either Dirichlet or Neumann: $C \to 0$ or $\frac{\partial C}{\partial x} \to 0$ as $\mathbf{x} \to \infty$.

Since Eq.2 is a linear partial differential equation, we can use the principle of superposition to write the solution with the specified source term:

$$C(x,t) = \int d\tau d\mathbf{x}' G(\mathbf{x} - \mathbf{x}', t - \tau) Q(\mathbf{x}', \tau). \tag{3}$$

Here $G(\mathbf{x}, t)$ is the Green's function of the diffusion-advection equation, describing solution with a point (both in space and time) source of unit strength:

$$\frac{\partial G}{\partial t} = D_x \frac{\partial^2 G}{\partial x^2} + D_y \frac{\partial^2 G}{\partial y^2} - u_x \frac{\partial G}{\partial x} + \delta(x)\delta(y)\delta(t). \tag{4}$$

Here, the source is located at $\mathbf{x}_s = (0, 0)$, and it is active at $t_s = 0$.

In our case, Q is a combination of several point sources, which (with the help of the properties of the delta function) allows us to replace the integral in Eq.3 with a sum over them:

$$C(\mathbf{x}, t) = \sum_{s=1}^{N_s} G(\mathbf{x} - \mathbf{x}_s, t - t_s) Q_s. \tag{5}$$

Here, N_s is the total number of sources, and Q_s is a constant contaminant mass release that specifies the strength of the s-th source at time t_s and location $\mathbf{x}_s$. The Green's function for Eq.4 is well known [21], and can be written as:

$$G(\mathbf{x}, t) = \frac{1}{4\pi\sqrt{D_x D_y} t} e^{-\frac{(x - u_x t)^2}{4 D_x t}} e^{-\frac{y^2}{4 D_y t}}. \tag{6}$$

where x and y are the components of the vector $\mathbf{x}$ and $t > 0$ (again, note that this implies a specific choice for the advection velocity $\mathbf{u} = (u_x, 0)$). Apparently, $G(\mathbf{x}, t)$ trivially satisfies the boundary condition at infinity.

It is important to note that despite the fact that here we are considering explicitly only point sources, the developed method we will introduce in the next sections can be straightforwardly applied to sources with more complicate space and time dependencies: $Q \sim \sum f^{(s)}(\mathbf{x}, t)$. In this case, according to the general principle of superposition [18, 22], the solution of Eq.2 can be written as:

$$C(\mathbf{x}, t) = \sum_{s=1}^{N_s} \int d\mathbf{x}' d\tau G(\mathbf{x} - \mathbf{x}', t - \tau) f^{(s)}(\mathbf{x}', \tau). \tag{7}$$

The above integral over the source time and spatial coordinates (with known functional dependence $f(\mathbf{x}, t)$) can be solved analytically, and the result for $C(\mathbf{x}, t)$ reduces to a closed-form expression (cf. [22, 21]). But even if this is not the case, the method we discuss in the rest of the paper will work for $C(\mathbf{x}, t)$ obtained using a numerical integration.

2.2. Blind Source Separation (BSS) methods

In the typical BSS problem [15], the observed data, V, ($V \in M_{n,m}(R)$), is formed by a linear mixing (at each one of the n detectors) of d unknown original signals, H, ($H \in M_{d,m}(R)$), blended by an also unknown mixing matrix, W, ($W \in M_{n,d}(R)$), i.e.,

$$V_n(t_m) = \sum_d W_{n,d} H_d(t_m) + \epsilon, \tag{8}$$

where $\epsilon \in V_{n,m}(\mathbb{R})$, and denotes presence of possible noise or unbiased errors in the measurements (also unknown). If the problem is solved in a temporally discretized framework, the goal of a BSS algorithm is to retrieve the d original signals (sources), H, that have produced n observation records, V, at t_m discretized moments in time, at which the signals are recorded at the detectors. Since both factors H and W are unknown (the size d of these matrices is also unknown, because we do not know how many sources have been mixed at each detector record), the main difficulty in solving a BSS problem is that it is under-determined.

There are two widely-used approaches to resolve this BSS underdetermination: Independent Component Analysis (ICA), [23, 24], and Non-negative Matrix Factorization (NMF), [25, 16]. ICA presupposes a statistical independence of the original signals and thus aims to maximize the non-Gaussian characteristics of the estimated sources in H. The other approach, NMF, is

a unsupervised learning method, created for parts-based representation, [26] in the field of image recognition, [25, 16], that was successfully leveraged for decomposition of mixtures formed by various types of signals [27]. In contrast to ICA, NMF does not seek statistical independence or constrain any other statistical properties (i.e., NMF allows the original sources to be partially correlated); instead, NMF enforces a non-negativity constraint on the original signals in H and their mixing components in W. NMF can successfully decompose large sets of non-negative additive observations, V, by leveraging the multiplicative update algorithm [16]. However, the original NMF algorithm requires *a priori* knowledge of the number of the original sources.

Recently, we reported a new methodology, we called NMFk, where the coupling of the original NMF algorithm with a custom semi-supervised clustering based on k-means algorithm that allows us to identify the unknown number of sources based on the robustness of the solutions. The machine learning part of the developed here new hybrid method, Green-NMFk, is following the ideas of NMFk originally reported in [17].

2.3. The hybrid method Green-NMFk

If we wanted to calculate the signal at a given detector location, composed as a mixture of signals from a set of known sources the explicit form of the Green's function, (Eq.6) could be enough to solve the problem. However, we are aiming to solve a more complicated inverse problem: to determine the characteristics of an *unknown number* of sources based on their mixed signals recorded by multiple detectors. Since this type of problems is known as BSS problems, and the signals are non-negative, at a first glance NMF appears as a good match for our task, moreover the multiplicative algorithm utilized by NMF is very efficient and powerful. Yet, despite their advantages, none of the direct BSS based methods is directly appropriate for our task. The issue is in the nature of the process of contaminant transport itself.

Indeed, while some physical processes (e.g., dispersionless processes subject to wave equation) could permit signals that keep their form undistorted as they travel through the medium, the parabolic equation describes diffusion. To examine the consequences of this, let us consider a single point source. Detectors situated at different distances from the source will record distinct signals, differing in shape and time dependence (this is easy to deduce from the general form of the Green's function in Eq.6). This distortion is difficult to be treated by the BSS methods by themselves. Indeed, there is

an NMF method, the so-called convolute NMF [28], that could be applied in this case, however, its algorithm does not take advantage of the knowledge of the diffusion processes involved in the contamination problem, and hence the reconstruction of the original signals would not necessarily resemble straightforwardly the solution of the advection-diffusion equation. Furthermore, this method will not provide insights about the physics parameters impacting the signal propagation through the medium.

The hybrid method, we are proposing here, takes advantage of our knowledge of the physical processes involved in the signal formation by using the explicit form of the Green's function of the advection-diffusion equation (unlike the typical BSS methods, which are model-free methods). We would also apply our previously developed NMFk protocol [17] for decomposition of the mixtures of contamination fields recorded by each detector and estimation of the (unknown) number of sources, based on their robustness.

Note that the issue of signals changing their form as they propagate is fairly common one, and applies to, for example, signals composed of dispersive waves. The method we present below can be used to treat these important problems as well, with a suitable change of the Green's function.

3. Methodology

In the previous section, we presented the problem and introduced some notations. In this section, we will focus on our approach to identifying the contaminant sources. The general method we propose in this work has two well-separated stages: (a) Nonlinear minimization and (b) NMFk-type estimation of the unknown number of sources based on the robustness of the solutions.

3.1. Nonlinear minimization

The first step in our method is a nonlinear minimization. Based on the Green's function of advection-diffusion equation, we know the explicit form of the original signals at times t_q, $q = 1, 2, .., t_{max}$ and at the locations of each of the n detectors $(x_p,\, y_p)$, $p = 1, 2, .., n$. These signals originate from N_s sources, located at the point locations $(x_i,\, y_i)$, $i = 1, 2, ..., N_s$, with source strengths Q_i. Therefore, we have to solve a NMF-type of equation like:

$$V_p(t_q) = \sum_{i=1}^{N_s} W_i H_{i,p}(t_q) + \epsilon; q = 1, 2, .., t_{max} \tag{9}$$

where,

$$W_i \equiv Q_i, \tag{10}$$

$$H_{i,p}(t_q) = \frac{1}{4\pi\sqrt{D_x D_y}t_q} e^{-\frac{((x_i-x_p)-u_x t_q)^2}{4D_x t_q}} e^{-\frac{(y_i-y_p)^2}{4D_y t_q}}. \tag{11}$$

and ϵ is the Gaussian noise or unbiased measurement errors. As explained earlier, the signal at each detector is a superposition of contributions from all N_s sources (note that depending on source/detector locations the contribution of some of the sources may be negligible). Although we know the coordinates of each of the detectors, $(x_p,\ y_p)$, $p = 1, 2, .., n$, and for each individual source we know the functional form of its Green function, G_i, $i = 1, 2, .., N_s$, the physical parameters, Q_i, x_i, and y_i characterizing the contaminant sources and the contaminant transport characteristics u_x, D_x, and D_y are still unknown. The goal of the minimization procedure is to obtain the physical parameters and transport characteristics, which reproduce (with some accuracy) the observed data, rather than just reconstruct unknown functional dependence in space and time. This considerably simplifies the problem, and for many cases the minimization can be carried by well-known nonlinear least-squares procedures (for example, Levenberg-Marquardt [29]) as implemented in the LANL's open source MADS (http//mads.lanl.gov; [30, 31]) and applied to minimize the cost function O,

$$O = \sum_{p=1}^{n} \sum_{q=1}^{t_{max}} \left(V_{p,q} - \sum_{d=1}^{N_s} W_d H_{d,p,q} \right)^2 = ||V - W * H||_{NLS} \tag{12}$$

The minimization of this cost function assumes that each measurement at a given space-time point is independent Gaussian-distributed random variable, which correspond to the white noise, ϵ. If each detector has its own and different (possibly time-dependent) measurement error, minimizing the cost function in Eq.12 should be replaced by a weighted least-squares procedure, where the cost at each point is weighed by the inverse square of its measurement error.

Note that since Gaussian functions form basis in the functional space, none of them can be presented as a linear combination of each other, which guarantees an uniqueness of the minimum of the cost function in (Eq.12).

However, there is one parameter that cannot be extracted directly by minimization of O in Eq.12: This parameter is the unknown number of

contamination sources N_s, which we need to consider in the explicit form of the solution.

To identify the unknown number of the original sources, N_s, we leverage our NMFk protocol [17].

3.2. NMFk

If we know the number of sources N_s, the first step described in the previous section would be all that is needed: from the best solution of the minimization procedure (with known N_s), we would extract the desired estimates of the physical parameters, and thus solve the inverse problem. Unfortunately, the true number of sources is typically unknown, and we have to identify this parameter from the observations. However, the solution of Eq.12, is based on some (often inaccurate) initial guess for the unknown parameters. A naive approach would be to explore all of the possible solutions applying the nonlinear minimization described in the previous section for a range of possible number of sources. Then the solution with the smallest reconstruction error will eventually identify the number of sources, N_s. However, this is obviously a flawed approach – the over-fitting will certainly lead to an over-estimation of the number of sources: more free parameters will generally lead to a better fit, irrespective of how close the estimated number of sources is to the real one.

The original NMF also requires *a priory* knowledge of the number of the original sources. Previously, by coupling the NMF with a custom semi-supervised clustering, we have demonstrated that the number of the original sources can be estimated based on the robustness and reproducibility of the solutions [17]. This approach was introduced to decompose the largest available dataset of human cancer genomes [32], and then extended for decomposition of physical signals/transients [17].

Specifically, the NMFk protocol explores consecutively all possible numbers of original sources, $i = 1, 2..., d$, and then estimates the accuracy and robustness of the solutions with different number of sources. Thus, NMFk performs d sets of M simulations, called runs, where each run is using different number of sources, $i = 1, 2, ..., d$, with random initial guesses for the unknown parameters. At the end of each run, we result with a set of M solutions, U_d, where each solution contains two matrices, H_d^j, W_d^j, (for d original sources, and $j = 1, 2, ..., M$),

$$U_d = ([H_d^1; W_d^1], [H_d^2; W_d^2], ..., [H_d^M; W_d^M]) \tag{13}$$

After that, NMFk leverages a custom semi-supervised clustering to assign each of these M solutions in a given set U_d to one of d specific clusters. This custom semi-supervised clustering is a k-means clustering that, however, keeps the number of solutions in each cluster equal. For example, for the case of $d = 2$, after a run with $M = 1,000$ simulations (performed with random initial guesses for the unknown parameters), each of the two clusters will contain $1,000$ solutions. Note that we have to enforce the condition that the clusters are with equal number of solutions, since each NMF simulation contributes equal number of solutions for each source. During clustering the similarity between sources h_1 and h_2 is measured using the cosine distance (also known as cosine similarity) [33], $\rho(h_1, h_2)$,

$$\rho(h_1, h_2) = 1 - \frac{\sum_{i=1}^{m} h_{1,i} h_{2,i}}{\sqrt{\sum_{i=1}^{m} {h_{1,i}}^2} \sqrt{\sum_{i=1}^{m} {h_{2,i}}^2}} \tag{14}$$

The main idea for estimating the unknown number of sources is to use the separation between the clusters as a measure of how good is the particular choice of d as the number of the unknown sources. In the case of the under-fitting, for solutions with d less than the actual number of sources, N_s, we expect that the clustering would be good; several of the sources could be combined to produce one "super-cluster". However, clustering will break down significantly in the case of over-fitting, when d exceeds the true number of sources, N_s. Indeed, in this case, even if the reconstruction error of the solution is small, we do not expect the solutions to be well clustered, since there is no unique way to reconstruct well the solutions with $d > N_s$, and at least some of the clusters will be artificial, rather than real entities. Thus, the quality of the clustering can be used as an indicator of the solution robustness and applied to identify the number of sources. Hence, we estimate the degree of clustering for different number of sources, and plot it as a function of d, and we expect a drop after d crosses the N_s value [17].

To quantify this behavior, after the clustering, we compute the Silhouette widths [34] of the clusters, and construct the average Silhouette width, which is a measure of how well the solutions are clustered (i.e., reproduced) if we consider d original sources.

In addition to the average Silhouette width, we use the NLS reconstruction error (Eq.12) to evaluate the accuracy with which the average solutions, that is, the derived centroids of the clusters $[H_d^a; W_d^a]$ reproduce the observations V. In general, the solution accuracy increases (while the solution

robustness decreases) with the increase of the number of unknown sources. Hence, the average Silhouette width and the average reconstruction error for each of the d cluster solutions can be used to estimate the optimal number of contaminant sources, N_s.

Specifically, we select N_s to be equal to the number of sources that accurately reconstruct the observations (i.e., their average reconstruction error is small enough) and whose clusters of solutions are sufficiently robust (i.e., their average Silhouette width is close to 1).

This condition can be formulated with the help of the Akaike Information criterion (AIC) [35]. To calculate AIC, we take all possible numbers of sources that lead to a Silhouette width above certain threshold (for example, 0.7). Then, we compare these models by calculating (for each number of sources d) the value:

$$AIC = 2d - 2\ln(L) = 2d + N\ln\left(\frac{O^{(d)}}{N}\right),$$

where L is the likelihood functions of the model with given d, and we define it using the average reconstruction error $O^{(d)}$ of the solutions we have kept in the clustering procedure for this particular d: $\ln(L) = -(N/2)\ln(O^{(d)}/N)$ ($N = n * m$, is the total number of data points; the product of the number of detectors n by the number of time observations m). The AIC is a standard measure of the relative quality of statistical models, which takes into account both the likelihood function (in our case determined by the average reconstruction error) and the degrees of freedom needed to achieve this level of likelihood (number of sources). Choosing the model that minimizes AIC helps avoid over-fitting.

Based on this approach, we have developed the Green-NMFk algorithm for identifying the number and characteristics of contaminant sources subject to advection-diffusion equation.

4. Results

4.1. Green-NMFk test workflow

Below is the summary of the main steps of the analyses performed to test our methodology:

1. *Generate the observation matrix*: For a given setup of the detector locations (e.g., Fig.1A and B), as well as for the chosen (in principle

arbitrary) values for u, D_x, D_y, source locations and source strengths Q_s, generate a synthetic dataset (matrix) for a discrete set of observation times for each detector. To do so the concentration transients generated from each source are computed using an analytical solution [21, 30] and the predicted concentrations for each detector are added into a matrix representing the mixtures of the N_s sources within the contamination plume at each of the n detectors.

2. *Obtain solutions*: For a series of d values ($d = 1, ..., n$), perform some large number, M, of NLS simulations with random initial values, to obtain d sets U_d, each with M solutions. To obtain solutions with smallest reconstruction error at a reasonable computational cost, we have developed the following algorithm. If in the first M_1 ($M_1 > 500$) simulation, there are solutions with reconstruction error less than 0.1% (or some other predetermined value), we run simulations until at least 20 such solutions are found. If there are no acceptable solutions in the first M_1 of them, we run the simulation for a fixed large number of times (here $> 10,000$).
3. *Cluster the solutions*: For each d value, we cluster a subset of the M solutions (keeping those that reconstruct the observations relatively well, determined by the relative norm of the solution). If we have solutions with reconstruction error less than 0.1%, we only cluster them, calculate the average Silhouette width and go to the next step. If we do not have any solutions that reconstruct the observations with our acceptance criterion, we take the first 20% of the solutions, sorted by the way how well they reconstruct the observations, and cluster them iteratively: we remove a fixed (small) percent of the worst solutions (outliers), cluster the remaining ones and compute the average Silhouette width. Next, we repeat the previous step until one (or more) of the following conditions are met: (i) the average Silhouette width is high (> 0.95); (ii) the average Silhouette width decrease significantly at the new step; (iii) there is only a small number (less than 20) of solutions left in each cluster.
4. *Determine N_s*: For each d value, we graphically analyze the average Silhouette width and average reconstruction NLS error (Eq.12) of the obtained solutions, in order to find the optimal number, N_s, of original unknown sources. To automate the process and to make the choice of N_s more robust, we use also AIC.

5. *Extract the physical parameters*: Once N_s is estimated, extract the parameters for each source, by taking the centroids of the clusters with $d = N_s$.
6. *Validate the results*: To make sure the obtained parameters (including the number of sources) provide a reasonable estimate of the observations, we take two additional validation steps. First, we use the estimated parameters to compare the calculated and observed state variables (concentrations) at each detector. Second, we also verify that each one of the sources contribute reasonable portion (more than 1%) to the signal detected by at least one detector; this is a good way to check against over-fitting.

The constraints in this workflow can be further optimized depending on the nature of the solved problem without any lost of generality of the algorithm proposed above.

4.2. Synthetic Data

To illustrate our method, we apply Green-NMFk to identify sources from four synthetic data sets. For this purpose, we consider two general detector/source configurations (represented in Fig.1). For the first setup (presented on Fig.1A, the detector coordinates are: $D1 = (0.0, 0.0)$, $D2 = (0.5, -0.5)$, $D3 = (0.5, 0.5)$, $D4 = (-0.5, -0.5)$, $D5 = (-0.5, 0.5)$, $D6 = (0.0, 0.5)$, $D7 = (0.0, -0.5)$, $D8 = (-0.5, 0.0)$, $D9 = (0.5, 0.0)$. The source coordinates in the first setup are: $S1 = (-0.3, -0.4)$, $S2 = (0.4, -0.3)$, $S3 = (-0.3, 0.5)$, and $S4 = (-0.1, 0.25)$, and all sources are releasing contaminants with constant concentration equal to 0.5 mg/L. In the second general configuration (Fig.1B), the source coordinates are: $S1 = (-0.9, -0.8)$, $S2 = (-0.1, -0.2)$, and $S3 = (-0.2, 0.6)$, with release concentrations: 0.5 mg/L, 0.7 mg/L, and 0.3 mg/L, respectively.

To make the problem more realistic, we set the physical parameters of the sources and the medium to be in ranges consistent to these observed at actual groundwater contamination sites. Thus, in both setups the distances are measured in kilometers, the advection velocity: $u = 0.05$ km/year, and its direction was chosen as the x-axis of the coordinate system. We have assumed a significant anisotropy in hydrological dispersion: $D_x = 0.005$ km/year^2 and $D_y = 0.00125$ km/year^2 (thus, $D_y/D_x = 0.25$, due to the presence of advection and mechanical dispersion). We also assume t_0 (the time of source activation) to be known, and take it for all sources to be -10 years (10

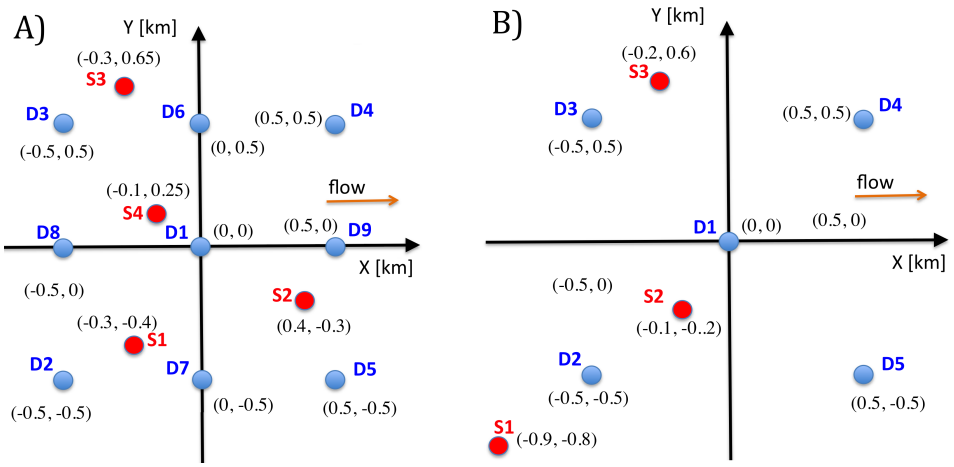

Figure 1: Test setups representing arrays of detectors (blue dots) and sources (red dots). On panel (A), there are nine detectors and four sources. On panel (B), there are five detectors and three sources.

years before the start of data collection). We consider a time span of 20 years (starting with $t = 0$), with measurements taken four times per year, so there is a total of 80 time points for each detector. Mixing the sources at each detector with added Gaussian noise with strength 10^{-3}, we construct four different observation sets (observational matrices) based on the two test setups presented in Fig.1.

To allow the minimization procedure to work on all data points simultaneously, we combine the observations in a single vector with $n \times m$ elements (n is the number of detectors and m is the number of time observations; $m = 80$). Further, we write a function which is a linear combination of N_s Green's functions (for N_s point sources), each with unknown coordinates x_s and y_s, and unknown strength Q_1, Q_2, Q_3, ... Q_{N_s}. Also unknown are the parameters of the medium u, D_x, and D_y. Starting with random values for the unknown parameters, the NLS minimization procedure is executed which adjust the values of the unknown parameters until the $l2$-norm of the cost function does not change appreciably, or the maximum number of iterations is reached. For each possible number of original sources ($d \leq n$), using the constructed observation matrices, we performed runs, each with $M \leq 10,000$ simulations. Then, following the workflow in Section 4.1, we gradually prune the simulations, guided by the quality of clustering.

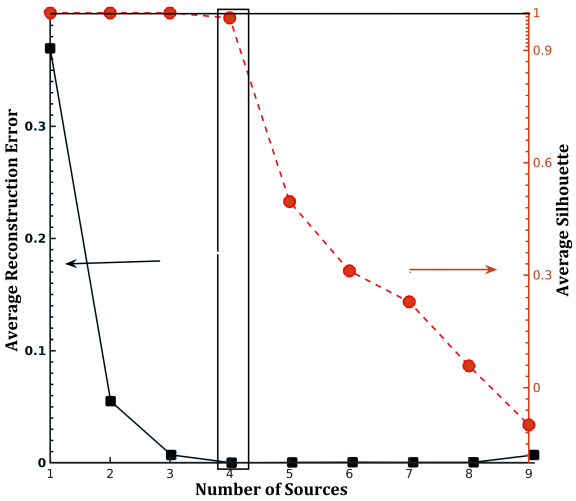

Figure 2: Average reconstruction error (black) and the average Silhouette width (red) of the solutions for the case of nine detectors and four sources. The rectangle outlines the results related to the optimal number of sources.

4.3. Green-NMFk results

The first setup (Fig.1A) has four point sources and nine detectors. In Fig.2, we demonstrate the average reconstruction error and average Silhouette width obtained for different number of unknown sources d. As it can be seen, the results unambiguously point to conclusion that there are four sources, $N_s = 4$. The average Silhouette width first slightly decreases as we move from one to three sources, while the reconstruction error remains relatively high; then the Silhouette width drop sharply as we go from four to five sources (Fig.2). With the increase of the number of sources from 4 to 5 and so on, we also observe that the reconstruction error remains almost the same, while the average Silhouette width of the clusters decreases. The values of the AIC function given in Table 1 also confirm this conclusion. The advection velocity estimated by the method is $u = 0.050214$ km/year, and the dispersion components are $D_x = 0.0050012$ km/year^2 and $D_y = 0.0012515$ km/year^2, These estimates are in very good agreement with the actual values ($u = 0.005$ km/year, $D_x = 0.005$ km/year^2 and $D_y = 0.00125$ km/year^2). The estimated source coordinates and strengths are given in Table 2 and are also very accurate.

The next three analyses are based on the second setup presented on Fig.1B.

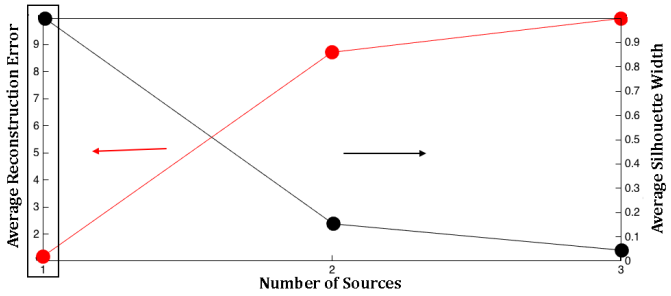

Figure 3: Average reconstruction error (red) and the average Silhouette width (black) of the solutions for the case of three detectors and a single source. The rectangle outlines the results related to the optimal number of sources.

First, we choose the second set to have only one point source, $S3$, with coordinates $(-0.2, 0.6)$ and strength $Q = 0.3$, and three detectors; $D3, D2, D4$. In Fig.3, we demonstrate the average reconstruction error and the average Silhouette widths obtained at the end of the procedure for different number of sources d. The method correctly selects only one source, and the values of the AIC function given in Table 1 confirm this choice. With the increase of the number of possible sources from 1 to 2 and then 3, we observe that the reconstruction error grows, while the Silhouette width of the clusters decreases. The methods yields for the advection velocity $u = 0.050125$ km/year, and for $D_x = 0.005002$ km/year^2 and $D_y = 0.0012475$ km/year^2. The source parameters provided in Table 2 also demonstrate a good agreement between the estimated and true parameter values.

Next, using another combination of sources, $S1$ and $S2$, and detectors $D1$, $D2$, $D3$, and $D4$ (Fig.1B), we again execute our algorithm. Again, the results convincing identify the correct number of sources, $N_s = 2$ (Fig.3). The Silhouette widths first slightly decrease as we move from one to two sources in our reconstruction procedure, and then drop sharply as we go from two to three (Fig.3). Combined with the accompanying increase in the reconstruction error between two and three source, this clearly points to two sources as the best estimate for N_s. The values of the AIC function, feasible with this conclusion, are given in Table 1. The estimated parameters are also very good: $u = 0.05224$ km/year, $D_x = 0.0050125$ km/year^2 and $D_y = 0.0012496$ km/year^2; Table 2 lists also the estimated strengths and the coordinates of the sources.

In our last test case, the signals are mixtures of all three sources, $S1$, $S2$,

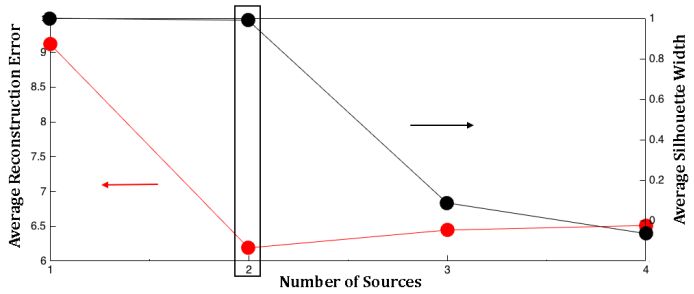

Figure 4: Average reconstruction error (red) and the average Silhouette width (black) of the solutions for the case of four detectors and two sources. The rectangle outlines the results related to optimal number of sources.

and $S4$, that are detected by each of the 5 detectors, forming the regular array on Fig.1B. As it can be seen in Fig.5, while the reconstruction error becomes quite small and flat for $N_s > 2$, the Silhouette width sharply drops for $d > 3$. Thus, the most robust answer for the unknown number of sources d is three. The medium parameters are: $u = 0.051341$ km/year, $D_x = 0.005132$ km/year^2, $D_y = 0.0012512$ km/year^2; Table 2 lists the source parameters.

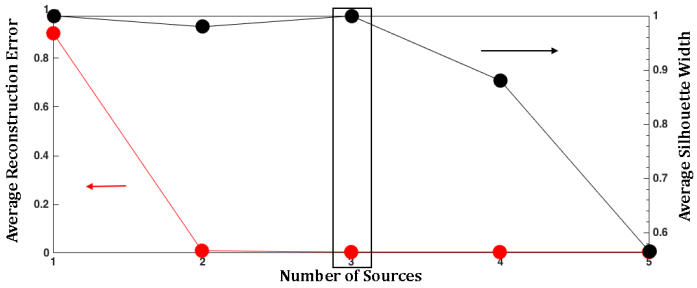

Figure 5: Average reconstruction error (red) and the average Silhouette width (black) of the solutions for the case of five detectors and three sources. The rectangle outlines the results related to optimal number of sources.

The values of the AIC function, are given in Table 1. Based on the results presented in Table 1 and the figures in this section, both the Silhouette width cut-off and the AIC criteria produced equivalent results for estimating the unknown number of sources. This is important observation considering that both metrics (Silhouette width and AIC) explore very different properties of the estimated solutions. The Silhouette width focuses on the robustness and

reproducibility of the solutions, while the AIC scores evaluates the solution parsimony.

The true and calculated parameters of the sources for all considered configurations are given in Table 2. From the values listed in the table, it can be seen that the Green-NMFk method is remarkably accurate, and the calculated coordinates are within ~ 2 % of their true values.

$AIC \times 10^{-3}$ estimates									
Case	d (unknown number of sources)								
	1	2	3	4	5	6	7	8	9
1 source 3 detectors	**-1.272**	(-0.734)	(-0.730)	na	na	na	na	na	na
2 sources 4 detectors	-1.138	**-1.260**	(-1.245)	(-1.240)	na	na	na	na	na
3 sources 5 detectors	-0.992	-4.257	**-4.512**	-4.511	(-4.508)	na	na	na	na
4 sources 9 detectors	-5.453	-6.821	-8.29.5	**-11.030**	(-10.904)	(-10.336)	(-10.019)	(-8.385)	(-8.222)

Table 1: AIC estimates for different unknown number of sources d for all the test cases. The values of d which are rejected because of bad clustering (Silhouette width < 0.7) are given in parentheses. Values of d which exceed the number of detectors are denoted as not applicable ("na").

Case	Source	Q mg/L		x km		y km	
		true	est.	true	est.	true	est.
1 source 3 detectors	#1	0.3	0.299	-0.2	-0.198	0.6	0.599
2 sources 4 detector	#1	0.5	0.511	-0.9	-0.899	-0.8	-0.801
	#2	0.7	0.704	-0.1	-0.100	-0.2	-0.200
3 sources 5 detectors	#1	0.3	0.297	-0.2	-0.201	0.6	0.597
	#3	0.5	0.499	-0.9	-0.899	-0.8	-0.744
	#3	0.7	0.704	-0.1	-0.097	-0.2	-0.199
4 sources 9 detectors	#1	0.5	0.502	-0.3	-0.300	0.4	0.400
	#2	0.5	0.499	-0.3	-0.300	-0.4	0.403
	#3	0.5	0.500	-0.3	-0.301	0.65	0.650
	#4	0.5	0.510	-0.1	-0.099	-0.25	0.249

Table 2: Green-NMFk results presenting estimated model parameters for 1, 2, 3 and 4 sources.

5. Conclusions

Our analyses demonstrate the applicability of the new hybrid method that couples machine-learning and inverse-analysis techniques. It is based on a NMF method for BSS combined with a custom semi-supervised clustering and the explicit form of the Green's function of the governing partial differential equation (PDE). The coupling between the Green's function solutions and the machine learning is based on iterative non-linear least-squares minimization procedure. We called this method Green-NMFk. The machine learning part of Green-NMFk (NMFk) is based on our previous work [17]. Green-NMFk is applied for identification of contaminant sources and PDE model parameters. In the synthetic tests, we generated datasets representing unknown contaminant sources detected as a set of mixed signals at a series monitoring wells (detectors). Using only these datasets, we correctly identified the number and location of the sources properties of the contaminant migration through the flow medium (advection velocity and dispersion coefficients). In presented analysis, our method correctly unmixed (deconstructed) the contamination fields (plumes) from the mixtures observed at the monitoring wells (detectors). It is assumed that each contaminant source is releasing the same geochemical constituent that is mixed in the aquifer, and the resultant mixture is detected at the observation points (detectors). The solved inverse problem is under-determined (ill-posed). To address this, the Green-NMFk algorithm thoroughly explores the plausible inverse solutions, and seeks to narrow the set of possible solutions by estimating the optimal number of contaminant source signals needed to robustly and accurately reconstruct the observed data. This allows us to estimate the unknowns: number of the contaminant sources, their locations, strengths, dispersivity, and advection velocity. Future work will include applying of the Green-NMFk to a real world data and probabilistic analyses of the uncertainty associated with the solutions identified by Green-NMFk.

The possible applications of the developed Green-NMFk approach are not limited to groundwater contamination problems. Various phenomena can be modeled by the diffusion equation, such as heat flow, infectious disease transmission, population dynamics, spreading chemical/biochemical substances in atmosphere, and many others. In general, the presented here method can be applied directly to any problem that is subject to partial-differential parabolic equation, where mixtures of an unknown number of physical sources are monitored at multiple locations. Green-NMFk can be also applied with differ-

ent equations with different Green's functions; for example, Green's function representing anomalous (non-Fickian) dispersion [36] or wave propagation in dispersive media. Finally, our Green-NMFk method was submitted as a part of our "Source Identification by Non-Negative Matrix Factorization Combined with Semi-Supervised Clustering," U.S. Provisional Patent App.No.62/381,486, filed by LANL on 30 August 2016.

6. Acknowledgements

This research was funded by the Environmental Programs Directorate of the Los Alamos National Laboratory. In addition, Velimir V. Vesselinov was supported by the DiaMonD project (An Integrated Multifaceted Approach to Mathematics at the Interfaces of Data, Models, and Decisions, U.S. Department of Energy Office of Science, Grant #11145687).

References

[1] L. W. Gelhar, Stochastic subsurface hydrology, Prentice-Hall, 1993.

[2] C. W. Fetter, C. Fetter, Contaminant hydrogeology, vol. 500, Prentice hall New Jersey, 1999.

[3] J. Guan, M. M. Aral, M. L. Maslia, W. M. Grayman, Identification of contaminant sources in water distribution systems using simulation–optimization method: case study, Journal of Water Resources Planning and Management 132 (4) (2006) 252–262.

[4] J. Atmadja, A. C. Bagtzoglou, Pollution source identification in heterogeneous porous media, Water Resources Research 37 (8) (2001) 2113–2125.

[5] V. Borukhov, G. Zayats, Identification of a time-dependent source term in nonlinear hyperbolic or parabolic heat equation, International Journal of Heat and Mass Transfer 91 (2015) 1106–1113.

[6] A. V. Mamonov, Y. R. Tsai, Point source identification in nonlinear advection–diffusion–reaction systems, Inverse Problems 29 (3) (2013) 035009.

[7] A. Hamdi, I. Mahfoudhi, Inverse source problem in a one-dimensional evolution linear transport equation with spatially varying coefficients: application to surface water pollution, Inverse Problems in Science and Engineering 21 (6) (2013) 1007–1031.

[8] J. Murray-Bruce, P. L. Dragotti, Spatio-temporal sampling and reconstruction of diffusion fields induced by point sources, in: 2014 IEEE International Conference on Acoustics, Speech and Signal Processing (ICASSP), IEEE, 31–35, 2014.

[9] C. W. Chan, G. H. Huang, Artificial intelligence for management and control of pollution minimization and mitigation processes, Engineering applications of artificial intelligence 16 (2) (2003) 75–90.

[10] A. Khalil, M. N. Almasri, M. McKee, J. J. Kaluarachchi, Applicability of statistical learning algorithms in groundwater quality modeling, Water Resources Research 41 (5).

[11] A. Rasekh, K. Brumbelow, Machine Learning Approach for Contamination Source Identification in Water Distribution Systems, in: World Environmental and Water Resources Congress, Palm Springs, CA, 2012.

[12] G. Manca, G. Cervone, The case of arsenic contamination in the Sardinian Geopark, Italy, analyzed using symbolic machine learning, Environmetrics 24 (6) (2013) 400–406.

[13] H. T. Shahraiyni, S. Sodoudi, A. Kerschbaumer, U. Cubasch, A new structure identification scheme for ANFIS and its application for the simulation of virtual air pollution monitoring stations in urban areas, Engineering Applications of Artificial Intelligence 41 (2015) 175–182.

[14] A. Vengosh, R. B. Jackson, N. Warner, T. H. Darrah, A. Kondash, A critical review of the risks to water resources from unconventional shale gas development and hydraulic fracturing in the United States, Environmental science & technology 48 (15) (2014) 8334–8348.

[15] A. Belouchrani, K. Abed-Meraim, J.-F. Cardoso, E. Moulines, A blind source separation technique using second-order statistics, IEEE Transactions on signal processing 45 (2) (1997) 434–444.

[16] D. D. Lee, H. S. Seung, Learning the parts of objects by non-negative matrix factorization, Nature 401 (6755) (1999) 788–791.

[17] B. S. Alexandrov, V. V. Vesselinov, Blind source separation for groundwater pressure analysis based on nonnegative matrix factorization, Water Resources Research 50 (9) (2014) 7332–7347.

[18] J. Bear, Dynamics of fluids in porous media, Courier Corporation, 2013.

[19] Y. Li, S. Osher, R. Tsai, HEAT SOURCE IDENTIFICATION BASED ONCONSTRAINED MINIMIZATION, Inverse Problems and Imaging 8 (1) (2014) 199–221.

[20] P. A. M. Dirac, The principles of quantum mechanics: vol 27 of The international series of monographs on Physics, 1958.

[21] E. Park, H. Zhan, Analytical solutions of contaminant transport from finite one-, two-, and three-dimensional sources in a finite-thickness aquifer, Journal of Contaminant Hydrology 53 (1) (2001) 41–61.

[22] E. J. Wexler, Analytical solutions for one-, two-, and three-dimensional solute transport in ground-water systems with uniform flow, US Government Printing Office, 1992.

[23] J. Herault, C. Jutten, Space or time adaptive signal processing by neural network models, in: Neural networks for computing, vol. 151, American Institute of Physics Publishing, 206–211, doi:10.1063/1.36258, 1986.

[24] S.-i. Amari, A. Cichocki, H. H. Yang, A new learning algorithm for blind signal separation, Advances in neural information processing systems 8 (1996) 757–763.

[25] P. Paatero, U. Tapper, Positive matrix factorization: A non-negative factor model with optimal utilization of error estimates of data values, Environmetrics 5 (2) (1994) 111–126.

[26] M. A. Fischler, R. A. Elschlager, The representation and matching of pictorial structures, Computers, IEEE Transactions on 100 (1) (1973) 67–92.

[27] A. Cichocki, R. Zdunek, A. H. Phan, S.-i. Amari, Nonnegative matrix and tensor factorizations: applications to exploratory multi-way data analysis and blind source separation, John Wiley & Sons, ISBN 978-0-470-74666-0, 2009.

[28] P. D. O'grady, B. A. Pearlmutter, Convolutive non-negative matrix factorisation with a sparseness constraint, in: 2006 16th IEEE Signal Processing Society Workshop on Machine Learning for Signal Processing, IEEE, 427–432, 2006.

[29] D. W. Marquardt, An algorithm for least-squares estimation of nonlinear parameters, Journal of the society for Industrial and Applied Mathematics 11 (2) (1963) 431–441.

[30] Vesselinov V. V., D. O'Malley, Y. Lin, S. Hansen, B. Alexandrov, MADS.jl: Model Analyses and Decision Support in Julia, URL `http://mads.lanl.gov/`, 2016.

[31] V. V. Vesselinov, D. O'Malley, Model Analysis of Complex Systems Behavior using MADS, in: AGU Fall Meeting, San Francisco, CA, 2016.

[32] L. B. Alexandrov, S. Nik-Zainal, D. C. Wedge, P. J. Campbell, M. R. Stratton, Deciphering signatures of mutational processes operative in human cancer, Cell reports 3 (1) (2013) 246–259.

[33] T. Pang-Ning, M. Steinbach, V. Kumar, Introduction to data mining, Addison-Wesley, ISBN 978-0321321367, 2006.

[34] P. J. Rousseeuw, Silhouettes: a graphical aid to the interpretation and validation of cluster analysis, Journal of computational and applied mathematics 20 (1987) 53–65.

[35] H. Akaike, Akaike?s Information Criterion, in: International Encyclopedia of Statistical Science, Springer, 25–25, 2011.

[36] D. O'Malley, V. V. Vesselinov, Analytical solutions for anomalous dispersion transport, Advances in Water Resources 68 (2014) 13–23, ISSN 03091708, doi:10.1016/j.advwatres.2014.02.006, URL `http://dx.doi.org/10.1016/j.advwatres.2014.02.006`.